Utilizing Adaptive Droop Control to Improve the Accuracy of Load Power Balancing in DC Nanogrid Batteries

Fourys Yudo Setiawan Paisey
Department of Electrical Engineering, Institut Teknologi Sepuluh Nopember, Indonesia | Department of Electrical Engineering, Universitas Papua, Indonesia
7022222014@student.its.ac.id

Adi Soeprijanto
Department of Electrical Engineering, Institut Teknologi Sepuluh Nopember, Indonesia
adisup@ee.its.ac.id (corresponding author)

Feby Agung Pamuji
Department of Electrical Engineering, Institut Teknologi Sepuluh Nopember, Indonesia
feby@ee.its.ac.id

Received: 28 March 2025 | Revised: 25 April 2025 | Accepted: 4 May 2025

 DOI: /https://doi.org/10.48084/etasr.11190

ABSTRACT

This paper proposes an independent and flexible control strategy for Battery Energy Units (BEUs) in autonomous DC Nano Grids (DCNGs) using a communication-based system. The proposed strategy employs a hierarchical control approach, where the primary control manages power balance among BEUs, while the secondary control mitigates DC bus voltage deviations caused by droop operation. This ensures optimal power distribution while considering line resistance variations, State of Charge (SoC), and virtual power levels. The method prioritizes BEUs with higher SoC to contribute more power to the load while reducing the burden on lower SoC units. Additionally, a voltage recovery technique is implemented to maintain DC grid voltage stability. Beyond technical improvements, these findings can contribute to more efficient energy management in decentralized renewable energy systems, supporting the scalability of sustainable nanogrid infrastructures in remote or off-grid communities. An additional advantage is that in the event of a failure in the control of BEU1, the control of the unaffected BEU remains operational, ensuring system continuity. A comprehensive simulation comparison between conventional and the proposed method was conducted in MATLAB/Simulink under varying load power conditions. The results demonstrate that the proposed control strategy significantly improves power balancing accuracy and voltage stability.

Keywords-DC nanogrid; Battery Energy Unit (BEU); hierarchical control; adaptive droop control

I. INTRODUCTION

The increasing adoption of Distributed Generators (DGs) as Renewable Energy Sources (RESs) is driven by concerns over environmental pollution and the depletion of fossil fuels. Among various solutions, DC nanogrids (DCNGs) have gained attention due to their ability to integrate RESs efficiently. Unlike AC nanogrids, DCNGs eliminate reactive power losses, harmonics, and synchronization issues, making them a more reliable and efficient alternative for energy distribution [1-5]. However, maintaining stable operation in DCNGs remains challenging due to power fluctuations from intermittent RESs. Battery Energy Units (BEUs) play a crucial role in mitigating these fluctuations, requiring efficient management strategies. BEU coordination involves two key aspects: (a) battery management at the cell level and (b) power balancing across multiple BEUs within the grid. Conventional power-sharing methods often fail to account for State of Charge (SoC) variations, line resistance, and virtual power levels, leading to suboptimal energy distribution.

The increasing integration of RESs in standalone DCNGs presents a challenge in ensuring balanced power sharing among distributed energy storage units. Practically, unbalanced energy flow can reduce battery lifespan and system reliability. Theoretically, existing control strategies often overlook dynamic adaptation to SoC variations. Thus, there is a compelling need for an adaptive control mechanism that

ensures both operational stability and efficient energy utilization.

To address these limitations, the proposed control strategy was implemented and simulated in MATLAB/Simulink. Validation was conducted by comparing its performance under multiple test scenarios, including varying line resistances and load power levels. The reliability of the method was assessed through repeated simulations with different initial conditions to ensure consistency in the power-sharing ratio and system voltage stability. The communication link maintains balanced current and SoC levels by enabling data exchange between converters and batteries.

A Battery Management System (BMS) is responsible for monitoring key parameters such as temperature, individual cell voltage, and SoC balance within each BEU. To equalize the SoC among battery cells connected to a standard DC-DC converter, balancing circuits have been proposed [6-8]. A method utilizing multiple parallel DC-DC converters to achieve uniform SoC across cells connected to a grid-tied inverter via serial connection is introduced in [9]. Authors in [10] present a synchronized DC-DC module using digital control techniques to enhance system integration. A two-level control framework is also proposed to maintain SoC equilibrium across different operating modes while implementing comprehensive energy management strategies. Several studies have explored cooperative power-sharing strategies among BEUs in DCNGs. A hierarchical control method was proposed in [11] for balancing power and energy distribution in standalone DCNGs, primarily by regulating BEU output based on ramp rate and capacity and a multi-tier energy management system was introduced to improve cost efficiency in [12]. However, neither [11] nor [12] specifically address SoC imbalance among BEUs, which can lead to overcharging or over-discharging. To mitigate this issue, droop control strategies have been developed to simultaneously balance SoC, power, and energy distribution [13-18]. The droop gain of BEUs in [17, 18] was dynamically adjusted using a natural exponential function of SoC, achieving effective SoC balancing in low-voltage DCNGs. However, these methods rely on a central controller, which introduces a single point of failure. In [15, 16] droop coefficients were modified inversely to an exponential function of SoC (SoC^n), where n represents the convergence factor. This approach successfully equalizes SoC among BEUs without requiring additional communication links. However, the optimal value of n is not explored, and the voltage drop inherent in droop control is not considered. An additional control mechanism was introduced in [17] to balance SoC among BEUs used in residential nanogrid applications. Other studies have shown that improving the accuracy of power sharing among photovoltaic modules is crucial for maintaining the stability and efficiency of BIPV systems, especially under partial shading conditions [19-21].

In autonomous DCNGs, RESs typically employ Maximum Power Point Tracking (MPPT) algorithms to maximize energy extraction. Consequently, RESs behave as current sources, while BEUs play a dual role in stabilizing the bus voltage and regulating power flow through charging and discharging operations. When RES generation exceeds the demand, BEUs absorb the excess power and switch to charging mode. Conversely, during power deficits, BEUs discharge to compensate for the shortfall.

A. Conventional Droop

In DCNGs, conventional droop control plays a crucial role in maintaining system stability and power balance. This control method regulates voltage levels by adjusting the power output of each source, ensuring proportional load sharing based on their rated capacities while keeping voltage deviations within acceptable limits. The droop control mechanism for DC nanogrids is formulated as follows [9]:

$$V_{ref-i} = V_n - d_i P_i \quad (1)$$

where V_{ref-i} represents the reference output voltage of the DC-DC converter for each BEU, V_n is the nominal voltage of the DCNG, d_i denotes the droop coefficient, and P_i is the BEU's output power (positive during discharge and negative during charge). The droop coefficient is determined by the maximum allowable bus voltage deviation (ΔV_{max}) and the rated power capacity (P_{rate-i}) of the BEU:

$$d_i = \frac{\Delta V_{max}}{P_{rate-i}} \quad (2)$$

While conventional droop control effectively allocates power among BEUs based on their power ratings, it does not account for the SoC during charging and discharging. This limitation may lead to unequal SoC distribution, reducing overall battery lifespan and efficiency [9].

B. SoC Estimation Method

The SoC of a battery is a critical parameter in energy storage systems, influencing power management strategies and overall system efficiency. In [22], the Coulomb counting method was employed to estimate SoC, as defined by:

$$\delta i_{C,j} = i_{C,j} - i_{C\,bat\,avg} \quad (3)$$

$$\Delta SoC_i = SoC_i - SoC_{avg} \quad \text{where } i=1,2 \quad (4)$$

$$SoC_i = SoC_i(0) - \int_0^t \frac{I_{bat,i}(t)}{C_{bat,i}} dt \quad (5)$$

where $i_{C,j}$ represents the output current of converter i (where i=1,2,…), $i_{C\,bat\,avg}$ denotes the average output current of all converters, $SoC_i(0)$ is the initial SOC of battery i, $C_{bat,i}$ refers to the capacity of battery i, and $I_{bat,i}$ represents the output current of battery i.

The Coulomb counting method tracks the charge and discharge cycles by integrating the battery current over time, providing an accurate estimation of SoC. However, this method is susceptible to measurement errors and requires periodic recalibration to maintain accuracy.

II. PROPOSED METHOD

We introduce a droop control technique using the Proportional-Integral (PI) control method within a hierarchical structure that combines primary and secondary control layers. This approach ensures proportional power distribution between batteries while maintaining system voltage stability.

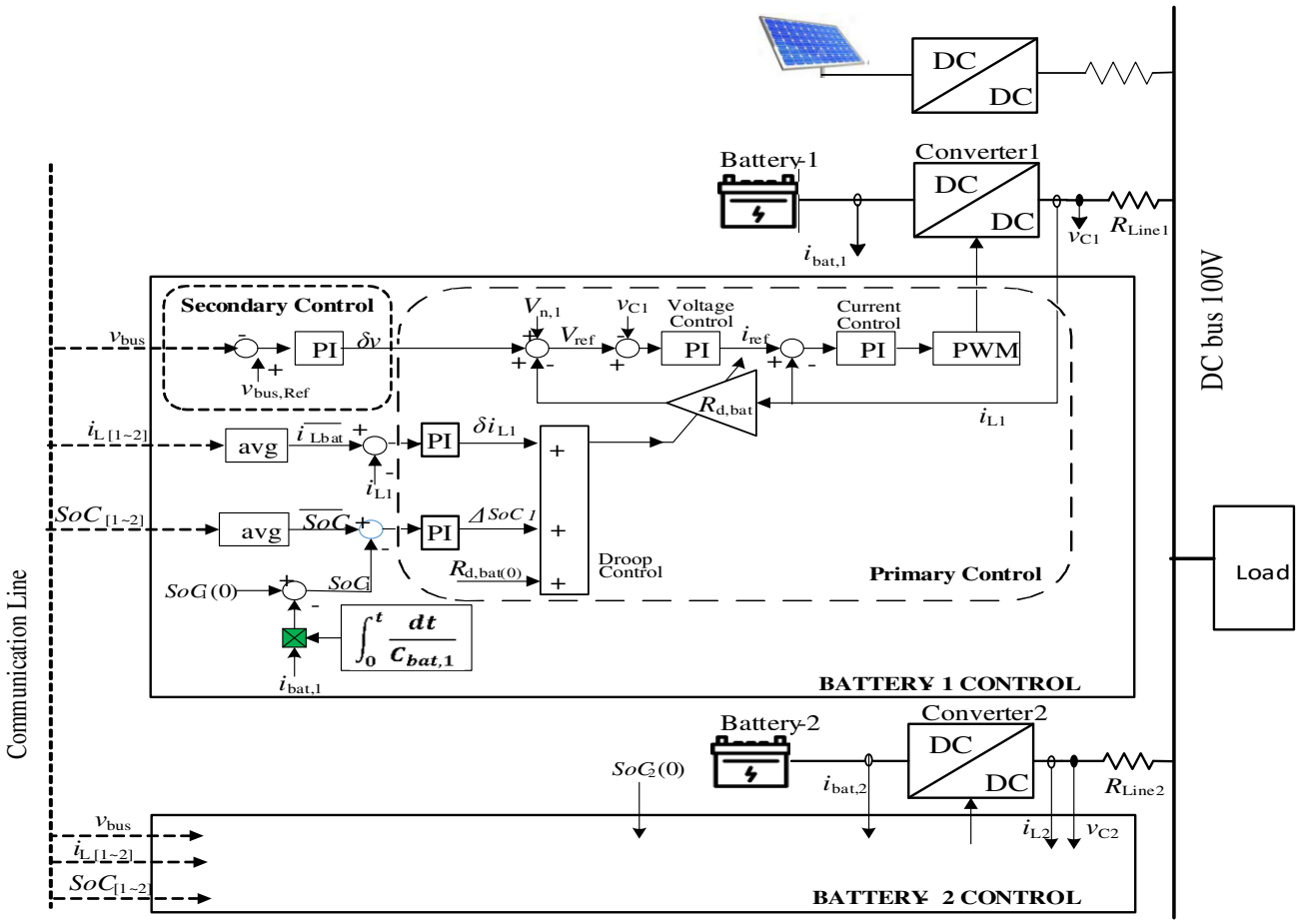

Fig. 1. Control diagram of the proposed power sharing and SoC balancing method.

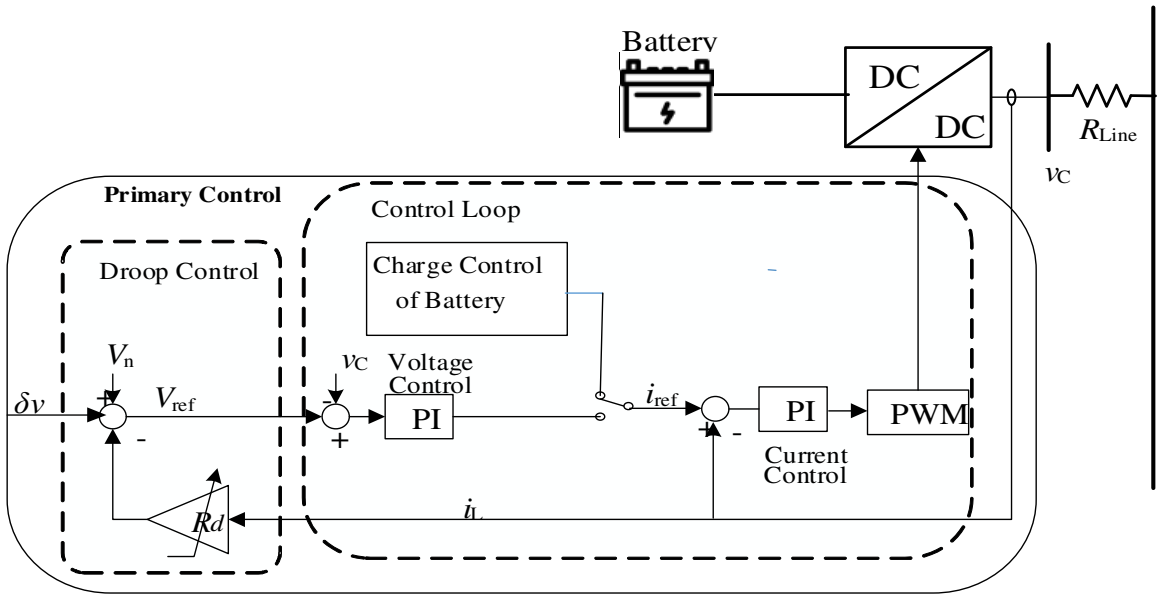

Fig. 2. Primary control diagram for power sharing between batteries.

A. Primary Control

Primary control is implemented using a cascade control strategy, consisting of an inner control loop for current regulation and an outer control loop that manages voltage control, droop control, and SoC control for the battery. The control diagram is presented in Figure 2. Adaptive droop control-voltage control, along with the outer control used by the battery converter, includes SoC control and adaptive droop control-voltage control. The battery's SoC control, which operates based on its SoC level, is illustrated in the control diagram (Figure 3).

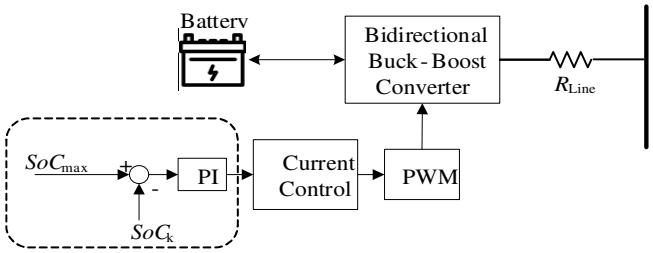

Fig. 3. SoC control diagram based on battery SoC level.

Figure 3 shows that the bidirectional buck-boost converter functions as a buck converter when the battery is in charging mode. The SoC control mode is activated when the battery reaches its maximum SoC (SoC_{max}), ensuring that the SoC remains at its maximum level. However, when $V_{bus} < V_{ref}$, the system switches to adaptive droop control mode for discharging, causing the bidirectional buck-boost converter to operate as a boost converter, as illustrated in Figure 4, which demonstrates that the bidirectional buck-boost converter in battery control can operate either in SoC control mode or in adaptive droop control mode, depending on the battery's SoC level and the DC bus voltage.

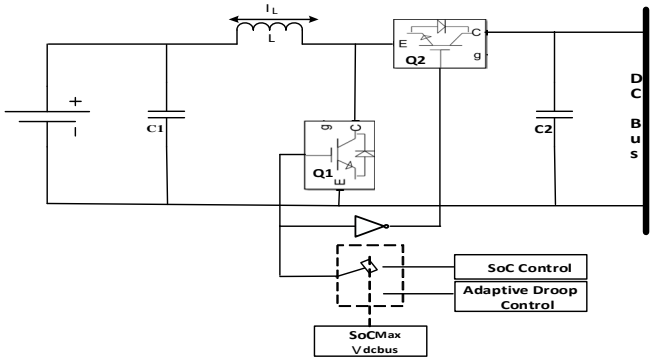

Fig. 4. Controlled bidirectional buck-boost converter circuit.

B. Secondary Control

One of the main drawbacks of the droop control method is the voltage deviation at the DC bus when there is an imbalance between the power generated and the power absorbed by the load. To mitigate this deviation, a PI control-based secondary control mechanism is implemented to compensate for the error (δv). Equation (6) is used to determine the error δv ($e_{\delta v}$). If an error $e_{\delta v}$ occurs, the PI controller calculates the correction value δv according to (7). This correction is then added to the initial voltage reference, allowing the DC bus voltage to be restored to the desired value, as expressed in (8). This process runs continuously to accommodate load variations and fluctuations in available power. Equation (8) has the same function as (1).

$$e_{\delta v}(t) = V_{bus} - V_{bus,ref} \quad (6)$$

$$\delta v = K_p\left(V_{bus} - V_{bus,ref}\right) + K_i \int \left(V_{bus} - V_{bus,ref}\right)dt \quad (7)$$

$$V_{ref} = V_{n,1} - (i_{L1}.R_{d,bat} + \delta v) \quad (8)$$

The reference voltage is updated based on the battery droop resistance, as shown in (9). The change in the SoC (ΔSoC) and the PI controller-corrected current adjustment are expressed in (10) and (11), respectively:

$$R_{d,bat} = \delta i_{L1} + \Delta SoC_1 + R_{d,bat}(0) \quad (9)$$

$$\Delta SoC_1 = k_P\left(SoC_{avg} - SoC_1\right) + \int \left(SoC_{avg} - SoC_1\right)dt \quad (10)$$

$$\delta i_{L1} = k_p\left(i_{bat\ avg} - i_{L1}\right) + k_I \int \left(i_{bat\ avg} - i_{L1}\right)dt \quad (11)$$

The change in Line 1 current (δi_{L1}) affects power distribution to the battery. A PI controller is used to adjust the Line 1 current (i_{L1}) to match the battery's average current ($i_{bat\ avg}$). The proportional component (k_P) immediately responds to the difference between $i_{bat\ avg}$ and i_{L1}. If i_{L1} is too high or too low compared to $i_{bat\ avg}$, an immediate correction is applied. The integral component (k_I) accumulates the error over time, eliminating steady-state errors and ensuring system stability by preventing long-term deviations.

$$SoC_1 = SoC_1(0) - \int_0^t \frac{i_{bat1}(t)}{C_{bat1}}dt \quad (12)$$

$$\Delta SoC_1 = k_P\left(SoC_{avg} - SoC_1\right) + k_I \int \left(SoC_{avg} - SoC_1\right)dt \quad (13)$$

Equations (12) and (13) describe how the PI control method adjusts SoC_1 to match the system's average SoC. The proportional component (k_P) directly responds to the difference between SoC_1 and the average SoC. If SoC_1 is lower than the average SoC, battery 1 will receive more power to compensate. Conversely, if SoC_1 is higher than the average SoC, battery 1 will either reduce its charging rate or increase discharging. The integral component (k_I) accumulates errors over time, preventing long-term deviations and ensuring a balanced power distribution between batteries. By gradually regulating SoC levels, the system maintains a balanced charge across all batteries, enhancing both efficiency and battery lifespan. The communication link ensures balanced current and SoC levels by exchanging data between converters and batteries.

III. RESULTS AND DISCUSSION

A. System Testing

An adaptive droop control simulation model was developed using the SimPowerSystem toolbox and the S-function block in MATLAB Simulink. In this topology, the load is connected to two BEUs, which serve as the main power sources, each with different SoC levels. The DC bus reference voltage is set to 100 V, and all converters operate at 50 kHz. The performance of the control system is evaluated by comparing traditional droop control, which uses a fixed droop resistance (R_d (0) = 1 Ω), with PI-based droop control. As shown in Figure 1, each BEU is interconnected with the others through a communication link. The simulated nanogrid DC system parameters are presented in Table I, while the DC-DC converter parameters are listed in Table II.

TABLE I. SYSTEM PARAMETERS

Parameters	Symbol	Value
Nominal DC Bus Voltage	V_{ref}	100 V
Maximum Battery SoC	SoC_{Bat}	98%
Battery Capacity	C_{Bat}	2.35 Ah
Line Resistance	R_{Line}	0.7 Ω, 0.2 Ω

TABLE II. DC-DC CONVERTER PARAMETERS

Converter	Parameters	Symbol	Value
Boost Converter	Input Voltage	V_{in}	48 V
	Output Voltage	V_{out}	100 V
	Switching Frequency	F_s	10 kHz
Buck-Boost Converter	Low Side Voltage	V_{low}	48 V
	High Side Voltage	V_{high}	100 V
	Switching Frequency	F_s	10 kHz

B. Test Scenario with BEU Charging and Static Load

The first test scenario was conducted in BEU charging mode with a fixed load of 200 W. The SoC was 97% for BEU1 and 96% for BEU2.

The test results indicate that conventional droop control fails to achieve a balanced load power distribution between the two BEUs. Even at the end of the test period, the power distribution remains unbalanced, as shown in Figure 5(c). In contrast, during the droop control test with PID, the load power distribution between the two BEUs reached equilibrium at t = 35 s (Figure 6(c)). The V-bus exhibited minor fluctuations (Figure 7(b)), while the battery charging current of BEU1 increased from t = 0 s to t = 33 s, as the system automatically adjusted the charging process until the SoC reached equilibrium. Meanwhile, BEU2 charged at a fixed rate, as illustrated in Figure 6(d).

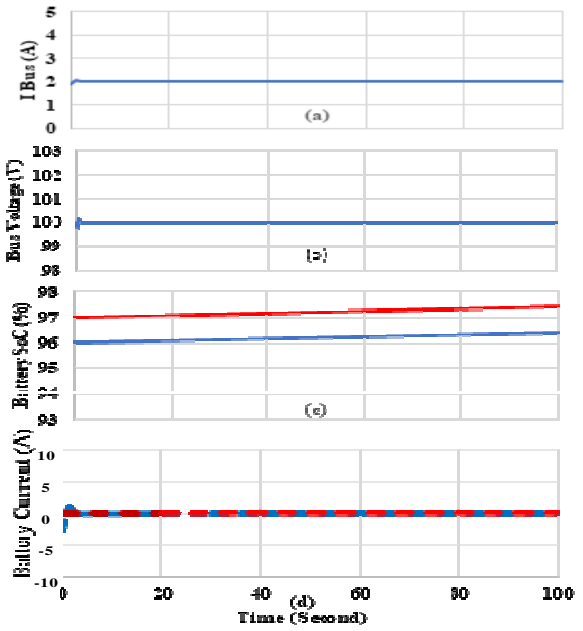

Fig. 5. Performance graph of convensional control with BEU charging and static load.

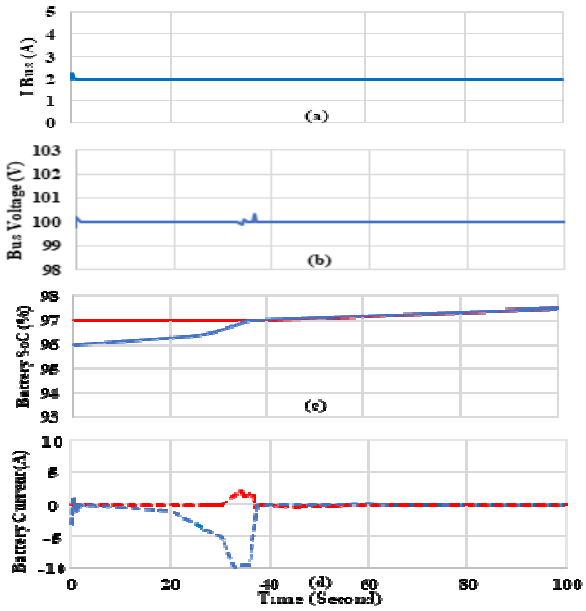

Fig. 6. Performance graph of adaptive droop PID control with BEU charging and static load.

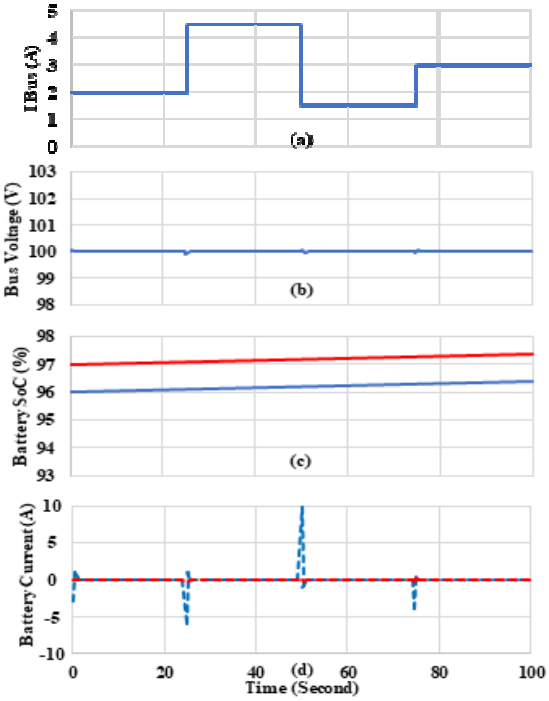

Fig. 7. Performance graph of conventional control with BEU charging and variable load.

C. Test Scenario with BEU Charging and Variable Load

In this test scenario, BEU1 and BEU2 operate in charging mode with SoC levels of 97% and 96%, respectively. The load varies over a 100-second period, alternating between 200 W, 450 W, 150 W, and 300 W. Simulation results indicate that the conventional droop control method fails to achieve a balanced load power distribution between the two BEUs (Figure 7(c)). In contrast, with PID-based droop control, the load power balance is achieved at t = 63 s. However, the bus-side voltage and current exhibit minor fluctuations due to load variations before stabilizing once the SoC levels of both BEUs reach equilibrium. The current stability of I-BEU1 is observed when the load is 200 W from t = 0 to t = 25 s. It then increases into the positive zone when the load rises to 450 W and drops into the negative zone when the load decreases to 150 W. Meanwhile, I-BEU2 enters the negative zone from t = 2 s to t = 45 s and stabilizes at t = 76 s (Figure 8(d)). In Figure 8(d), the positive zone represents the BEU supplying power to the DC bus, while the negative zone indicates the charging mode from the DC source. The zero point on the horizontal axis denotes the equilibrium between power supply and charging.

D. Test Scenario with BEU Discharging

The graphs illustrate two key conditions in the battery discharging process: one with a fixed load of 200 W and another where the load gradually changes from 200 W to 450 W, 150 W, and 300 W. In Figure 9, under a fixed 200 W load, the battery current remains relatively stable. The SoC difference between the two batteries gradually decreases over time due to the PI control, which adjusts current distribution. The bus voltage exhibits minor fluctuations but remains within nominal limits.

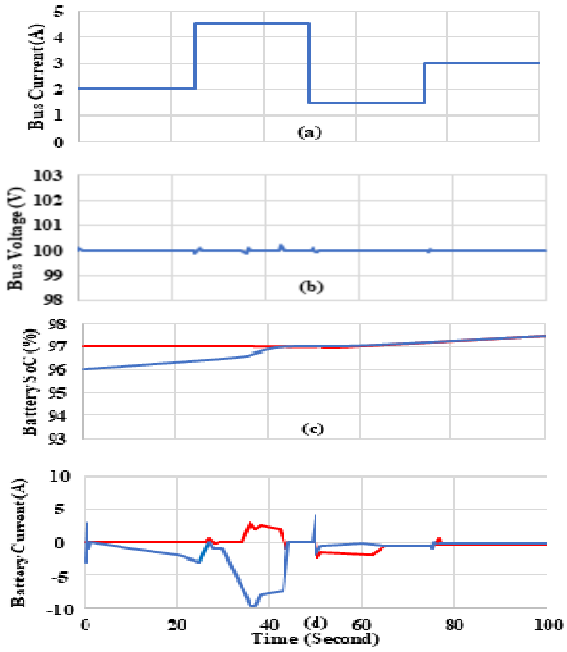

Fig. 8. Performance graph of adaptive droop PID control with BEU charging and variable load.

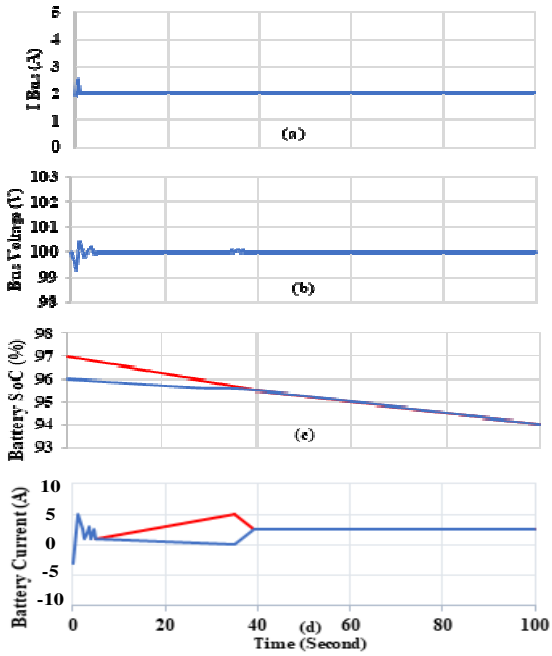

Fig. 9. Performance graph of adaptive droop PID control with BEU discharging and static load.

Figure 10 depicts the impact of load variations on system parameters. When the load increases from 200 W to 450 W, the bus current and battery current rise, causing a faster SoC drop.

Conversely, when the load decreases to 150 W, the battery current adjusts to maintain energy balance. Compared to the static condition, the bus voltage shows greater fluctuations, reflecting the system's response to load changes. The analysis results confirm that PI control accelerates SoC equilibrium between batteries during discharging, under both static and dynamic conditions. This control strategy enables more stable power distribution and an adaptive response to load variations, thereby improving the efficiency of the energy storage system.

The results suggest that adaptive droop control significantly improves power-sharing accuracy, which could reduce overcharging and overdischarging in real-world battery systems. This has practical implications for extending battery lifespan and optimizing energy distribution in remote microgrids. However, this study is limited to simulation-based validation and does not yet include hardware-in-the-loop testing. Compared to [15-17], who achieved 85% power-sharing accuracy using fixed droop, our method achieved near 100% accuracy under varying load conditions.

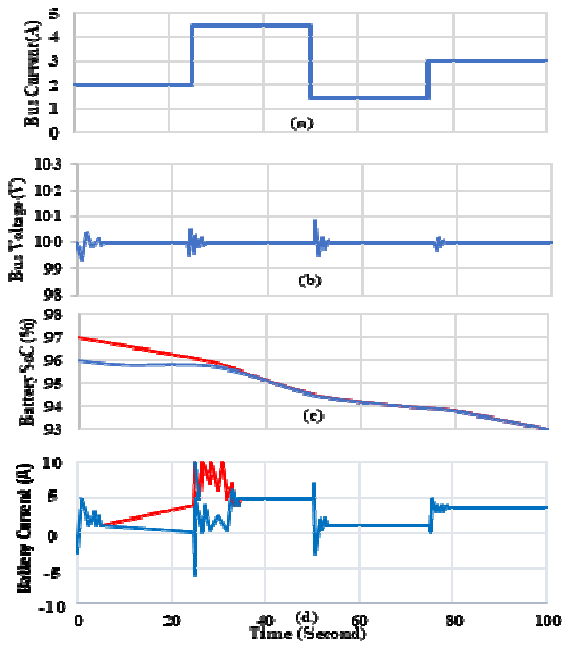

Fig. 10. Performance graph of adaptive droop PID control with BEU discharging and variable load.

IV. CONCLUSION

Simulation results conducted in MATLAB/Simulink demonstrate that the proposed method maintains a near-ideal power-sharing ratio of 1:1 between BEUs, even in the presence of variable line resistances and fluctuating load conditions. When compared to conventional droop control approaches, the proposed method exhibits significantly improved performance in terms of power-sharing precision and SoC equalization.

This study contributes to the advancement of control strategies for DC nanogrids by introducing a PI-based adaptive droop method that dynamically responds to state-of-charge disparities. This study enhances power-sharing accuracy and system stability, yielding superior results compared to prior research. It also establishes a strong foundation for future investigations into scalable and intelligent energy management systems in distributed energy environments. However, this study is limited to simulation-based validation and does not yet include hardware-in-the-loop testing.

ACKNOWLEDGMENT

The authors express their deepest appreciation to the Indonesian Endowment Fund for Education (LPDP) for providing financial support for this doctoral research.

REFERENCES

[1] F. Y. S. Paisey, A. Soeprijanto, and F. A. Pamuji, "Improving Load Power Sharing Accuracy in Standalone Microgrid DC Networks Using Intelligent Adaptive Droop Control Based on Fuzzy Logic Control," in *2023 International Conference on Radar, Antenna, Microwave, Electronics, and Telecommunications (ICRAMET)*, Bandung, Indonesia, Aug. 2023, pp. 190–195, https://doi.org/10.1109/ICRAMET60171.2023.10366745.

[2] J. M. Guerrero, J. C. Vasquez, J. Matas, L. G. de Vicuna, and M. Castilla, "Hierarchical Control of Droop-Controlled AC and DC Microgrids—A General Approach Toward Standardization," *IEEE Transactions on Industrial Electronics*, vol. 58, no. 1, pp. 158–172, Jan. 2011, https://doi.org/10.1109/TIE.2010.2066534.

[3] M. Fotopoulou, D. Rakopoulos, D. Trigkas, F. Stergiopoulos, O. Blanas, and S. Voutetakis, "State of the Art of Low and Medium Voltage Direct Current (DC) Microgrids," *Energies*, vol. 14, no. 18, Jan. 2021, Art. no. 5595, https://doi.org/10.3390/en14185595.

[4] A. T. Elsayed, A. A. Mohamed, and O. A. Mohammed, "DC microgrids and distribution systems: An overview," *Electric Power Systems Research*, vol. 119, pp. 407–417, Feb. 2015, https://doi.org/10.1016/j.epsr.2014.10.017.

[5] F. Dastgeer, H. E. Gelani, H. M. Anees, Z. J. Paracha, and A. Kalam, "Analyses of efficiency/energy-savings of DC power distribution systems/microgrids: Past, present and future," *International Journal of Electrical Power & Energy Systems*, vol. 104, pp. 89–100, Jan. 2019, https://doi.org/10.1016/j.ijepes.2018.06.057.

[6] D. Kumar, F. Zare, and A. Ghosh, "DC Microgrid Technology: System Architectures, AC Grid Interfaces, Grounding Schemes, Power Quality, Communication Networks, Applications, and Standardizations Aspects," *IEEE Access*, vol. 5, pp. 12230–12256, 2017, https://doi.org/10.1109/ACCESS.2017.2705914.

[7] Y. I. Mesalam, S. Awdallh, H. Gaied, and A. Flah, "Interleaved Bidirectional DC-DC Converter for Renewable Energy Application based on a Multiple Storage System," *Engineering, Technology & Applied Science Research*, vol. 14, no. 2, pp. 13329–13334, Apr. 2024, https://doi.org/10.48084/etasr.6944.

[8] N. Mukherjee and D. Strickland, "Control of Second-Life Hybrid Battery Energy Storage System Based on Modular Boost-Multilevel Buck Converter," *IEEE Transactions on Industrial Electronics*, vol. 62, no. 2, pp. 1034–1046, Oct. 2015, https://doi.org/10.1109/TIE.2014.2341598.

[9] K. D. Hoang and H.-H. Lee, "Accurate Power Sharing With Balanced Battery State of Charge in Distributed DC Microgrid," *IEEE Transactions on Industrial Electronics*, vol. 66, no. 3, pp. 1883–1893, Mar. 2019, https://doi.org/10.1109/TIE.2018.2838107.

[10] Y. Li and Y. Han, "A Module-Integrated Distributed Battery Energy Storage and Management System," *IEEE Transactions on Power Electronics*, vol. 31, no. 12, pp. 8260–8270, Sep. 2016, https://doi.org/10.1109/TPEL.2016.2517150.

[11] J. Xiao, P. Wang, L. Setyawan, and Q. Xu, "Multi-Level Energy Management System for Real-Time Scheduling of DC Microgrids With Multiple Slack Terminals," *IEEE Transactions on Energy Conversion*,

vol. 31, no. 1, pp. 392–400, Mar. 2016, https://doi.org/10.1109/TEC.2015.2488639.

[12] J. Xiao, P. Wang, and L. Setyawan, "Hierarchical Control of Hybrid Energy Storage System in DC Microgrids," *IEEE Transactions on Industrial Electronics*, vol. 62, no. 8, pp. 4915–4924, Dec. 2015, https://doi.org/10.1109/TIE.2015.2400419.

[13] C. Li, E. A. A. Coelho, T. Dragicevic, J. M. Guerrero, and J. C. Vasquez, "Multiagent-Based Distributed State of Charge Balancing Control for Distributed Energy Storage Units in AC Microgrids," *IEEE Transactions on Industry Applications*, vol. 53, no. 3, pp. 2369–2381, Feb. 2017, https://doi.org/10.1109/TIA.2016.2645888.

[14] N. L. Diaz, T. Dragičević, J. C. Vasquez, and J. M. Guerrero, "Intelligent Distributed Generation and Storage Units for DC Microgrids—A New Concept on Cooperative Control Without Communications Beyond Droop Control," *IEEE Transactions on Smart Grid*, vol. 5, no. 5, pp. 2476–2485, Sep. 2014, https://doi.org/10.1109/TSG.2014.2341740.

[15] T. R. Oliveira, W. W. A. Gonçalves Silva, and P. F. Donoso-Garcia, "Distributed Secondary Level Control for Energy Storage Management in DC Microgrids," *IEEE Transactions on Smart Grid*, vol. 8, no. 6, pp. 2597–2607, Aug. 2017, https://doi.org/10.1109/TSG.2016.2531503.

[16] X. Lu, K. Sun, J. M. Guerrero, J. C. Vasquez, and L. Huang, "Double-Quadrant State-of-Charge-Based Droop Control Method for Distributed Energy Storage Systems in Autonomous DC Microgrids," *IEEE Transactions on Smart Grid*, vol. 6, no. 1, pp. 147–157, Jan. 2015, https://doi.org/10.1109/TSG.2014.2352342.

[17] T. Dragičević, J. M. Guerrero, J. C. Vasquez, and D. Škrlec, "Supervisory Control of an Adaptive-Droop Regulated DC Microgrid With Battery Management Capability," *IEEE Transactions on Power Electronics*, vol. 29, no. 2, pp. 695–706, Oct. 2014, https://doi.org/10.1109/TPEL.2013.2257857.

[18] Q. Yang, L. Jiang, H. Zhao, and H. Zeng, "Autonomous Voltage Regulation and Current Sharing in Islanded Multi-Inverter DC Microgrid," *IEEE Transactions on Smart Grid*, vol. 9, no. 6, pp. 6429–6437, Aug. 2018, https://doi.org/10.1109/TSG.2017.2712658.

[19] D. Sarkar and P. K. and Sadhu, "Critical Comprehensive Performance Analysis of Static BIPV Array Configurations to Reduce Mismatch Loss and Enhance Maximum Power Under Partial Shading," *IETE Technical Review*, vol. 40, no. 4, pp. 465–497, Jul. 2023, https://doi.org/10.1080/02564602.2022.2127944.

[20] S. Bhattacharya, P. K. Sadhu, and D. Sarkar, "Performance evaluation of building integrated photovoltaic system arrays (SP, TT, QT, and TCT) to improve maximum power with low mismatch loss under partial shading," *Microsystem Technologies*, vol. 30, no. 5, pp. 583–597, May 2024, https://doi.org/10.1007/s00542-023-05564-0.

[21] D. Sarkar and P. K. Sadhu, "Power Enhancement by Hybrid BIPV Arrays with Fewer Peaks and Reduced Mismatch Losses under Partial Shading," in *2023 3rd International Conference on Intelligent Technologies (CONIT)*, Hubli, India, Jun. 2023, pp. 1–6, https://doi.org/10.1109/CONIT59222.2023.10205941.

[22] M. Effendy, M. Ashari, and H. Suryoatmojo, "PV Generation-Energy Storage Coordination with Adaptive Droop Control in Isolated DC Microgrid," *International Journal of Innovative Computing, Information and Control*, vol. 19, no. 3, pp. 655–669, 2023, https://doi.org/10.24507/ijicic.19.03.655.